Pharm Res (2015) 32:3952–3964
DOI 10.1007/s11095-015-1755-6

RESEARCH PAPER

Comparative Evaluation of Two Methods for Preparative Fractionation of Proteinaceous Subvisible Particles—Differential Centrifugation and FACS

Björn Boll[1,3] • Emilien Folzer[1,2,3] • Christof Finkler[1] • Jörg Huwyler[3] • Hanns-Christian Mahler[2] • Roland Schmidt[2] • Atanas V. Koulov[1]

Received: 13 April 2015 / Accepted: 9 July 2015 / Published online: 21 July 2015

ABSTRACT

Purpose The goal of this study was to compare and evaluate two preparative techniques for fractionation of proteinaceous subvisible particles. This work enables future studies to address the potential biological consequences of proteinaceous subvisible particles in protein therapeutic products.

Methods Particles were generated by heat stress and separated by size using differential centrifugation and FACS (Fluorescence-activated cell sorter). Resulting fractions were characterized by size-exclusion chromatography, light obscuration, flow imaging microscopy and resonant mass measurement.

Results Here we report the optimization and comprehensive evaluation of two methods for preparative fractionation of subvisible proteinaceous particles into distinct size fractions in the range between 0.25 and 100 μm: differential centrifugation and FACS. Using these methods, well-defined size fractions were prepared and characterized in detail. Critical assessment and comparison of the two techniques demonstrated their complementarity and for the first time—their relative advantages and drawbacks.

Conclusions FACS and differential centrifugation are valuable tools to prepare well-defined size-fractions of subvisible proteinaceous particles. Both techniques possess unique and advantageous attributes and will likely find complementary application in future research on the biological consequences of proteinaceous subvisible particles.

KEY WORDS particle fractionation · particle size · protein aggregation · proteinaceous particles · subvisible particles

ABBREVIATIONS

AF4	Asymmetric flow field-flow fractionation
CCF	Central composite face-centered
DoE	Design of experiments
FACS	Fluorescence-activated cell sorter
FI	Flow imaging microscopy
FSC	Forward scattering
IgG	Immunoglobulin G
LO	Light obscuration
MAb I	Monoclonal antibody
PBS	Phosphate buffered saline
RMM	Resonant mass measurement
RSM	Response surface methodology
UV	Ultraviolet light

INTRODUCTION

Protein aggregation takes place to a certain extent in all biotherapeutic formulations. Concerns are often raised and debated with regards to the theoretical potential for aggregates to cause an immune response in patients (1,2). Because of possible biological consequences, such as immunogenicity or altered bioactivity and pharmacokinetics (1,3–5), particles of proteinaceous origin have recently received increased interest from industry, academia and regulators (6). However, an

Björn Boll and Emilien Folzer contributed equally to this work.

Electronic supplementary material The online version of this article (doi:10.1007/s11095-015-1755-6) contains supplementary material, which is available to authorized users.

✉ Atanas V. Koulov
atanas.koulov@roche.com

[1] Pharma Technical Development (Biologics) Europe, Analytical Development and Quality Control, F. Hoffmann-La Roche Ltd., Grenzacherstrasse 124, 4070 Basel, Switzerland

[2] Pharma Technical Development (Biologics) Europe, Pharmaceutical Development & Supplies, F. Hoffmann-La Roche Ltd., Basel, Switzerland

[3] Department of Pharmaceutical Sciences, Division of Pharmaceutical Technology, University of Basel, Basel, Switzerland

undisputed general link between relevant clinical endpoints such as immunogenicity and subvisible particles in biotherapeutic preparations is still elusive. To date, the available data from *in vitro* and *in vivo* experiments are often conflicting and fragmented, which impedes coming to sound general conclusions. A major caveat of the published studies to date is the use of complex mixtures of therapeutic protein monomer, various aggregates and particle populations spanning a large range of sizes and possibly including a variety of chemical variations. However, potential effects generated by individual species (*i.e.*, different size or modification) are difficult to delineate in such complex mixtures, as individual species are not easy to obtain. Studies using human interferon beta show that particles exposed to extreme artificial conditions *e.g.*, metal oxidation or adsorbtion to glass induced an immune response in an transgenic mouse model (7,8). Clinical data with different interferon beta products show an increased anti-drug antibody formation which cannot solely attributed to aggregates but also to formulation (can contain HSA), modifications in the primary sequence and impurities acting as adjuvants (9). Furthermore, a sound characterization of complex mixtures used in these and other studies is often technically difficult or not feasible. Additionally, it has not been routinely employed by many groups studying the effects of subvisible particles generated by artificial stress conditions in various biological *in vitro* or *in vivo* models.

Thus, the reliable preparation of particles of such discrete sizes and their detailed characterization may provide significant advantage in further researching distinct species of proteinaceous subvisible particles in relevant *in vivo* or *in vitro* test systems, possibly being able to identify specific subvisible species primarily relevant for a potential biological consequence, if occurring.

Aggregation can be induced by a wide variety of stress conditions (especially, when protein is not adequately stabilized), including temperature stress, mechanical stress such as shaking and stirring, pumping, pH stress and freezing and/or thawing stress (10). Such stresses can also lead to proteinaceous particles, which can be in the visible or subvisible size range (10). The effect of different types of stress on the induction of protein particles and aggregates, has been investigated extensively (6,11–14). Depending on the protein and applied stress the resulting proteinaceous particles can range in size from nanometers to hundreds of micrometers. To characterize (subvisible) particle sizes, several methods have been applied to date and are in further assessment. Size exclusion chromatography is usually used for separation of soluble oligomeric (*i. e.* dimeric up to tetrameric) protein aggregates in the nanometer range (15,16), and is incapable to measure protein particles. For larger protein aggregates (nanometers and submicron), the use of asymmetrical flow field-flow fractionation (AF4) has been employed to measure proteinaceous particles with sizes between 50 and 250 nm (17–19). However, the separation with AF4 and size exclusion chromatography leaves room for improvement in terms of size range and partition of protein aggregation. The separation of proteinaceous particles in a size range of 1 to 50 μm which was reported recently, utilized a fluorescence-activated cell sorter (FACS) (20). Centrifugation for fractionation has been used in various fields such as cell biology (21), bacteriology (22) or in the soil industry (23) where species in the nm-, μm- and mm-size range have been successfully separated. Commonly used centrifugation methods to fractionate nanoparticles (24,25), blood leukocytes (26), blood plasma and erythrocytes (27), cells (28), bacteria (22), DNA (29) or soils (30) implement sucrose gradient, cesium chloride gradient, iodixanol gradients or the use of Ficoll/Percoll. However, the use of gradients has been shown to lead to contamination with new chemicals or residuals in the sample (27).

FACS and centrifugation are two of the most promising techniques for fractionation of proteinaceous particles and a most recent report utilized versions of the two approaches to enrich proteinaceous particles for follow-up biological characterization (31). However, to date these methods have not been comprehensively studied and optimized protocols are not available. Here we report the production of several distinctly sized protein nano- and micrometer subvisible particle fractions using the methods: a) differential centrifugation separation and b) fractionation of particles using a FACS. Both methods enabled preparation of well-defined size fractions of proteinaceous subvisible particles using a model mAb, as well as their detailed characterization. The two approaches were examined in detail and the experimental parameters that influence particle isolation, fractionation resolution, fraction purity, yield and other attributes were carefully evaluated, which allowed for the first time detailed characterization and optimization of these two particle separation strategies. Finally, we provide an assessment of the relative advantages and shortcomings of the two techniques.

MATERIALS AND METHODS

Materials

One Roche proprietary IgG1 monoclonal antibody (MAb1) was used as model protein for these studies. The solution was filtered using 0.22 mm Millex GV (PVDF) syringe filter units (Millipore, Bedford, MA) before use.

Dulbecco's phosphate-buffered saline (DPBS) from GIBCO (Invitrogen, San Diego, California) was used when PBS is mentioned. Glycerol (for molecular biology, ≥99%) was purchased from Sigma Aldrich (St. Louis, Missouri, USA).

Stress Condition: Mechanical & Heat Stress

Thermal/shaking stress was applied using a Thermomixer fitted for 1.5 ml-tubes (Thermomixer Comfort, Eppendorf, Germany). 1 ml of the 25 mg/ml mAb1 solution was incubated for 3 min at 80°C with 1400 rpm shaking. The temperature was chosen as being way beyond the melting temperature of the mAb1 (data not shown). The sample was then resuspended by drawing in and emptying out using a disposable Norm-inject 5 ml luer lock silicone free syringe (HENKE SASS WOLF, Tuttlingen, Germany) with attached 27 G×$1^{1/2}$ needle (0.40×40 mm) (Braun, Melsungen, Germany) for 20 consecutive times, in order to homogenize the solution and the generated insoluble matter. The bulk solution was stored at −80°C after stressing. The sample was diluted with PBS to an optimal concentration of particles before fractionation using FACS.

Preparation of Subvisible Particles by Differential Centrifugation

A 5810R table-top centrifuge (Eppendorf, Germany) with a swing-bucket angle A-4-81 rotor (R=180 mm) was used for all centrifugation experiments.

1) Empirical approach: selection of centrifuge time/acceleration/volume/media, multi-step preparation

   For fraction 1 (centrifugation-F1), 100 µl of initial stressed sample was overlaid on the top of 1.7 ml glycerol solution (25% w/w) using a pipette. The eppendorf tube was then centrifuged for 180 s at 25×g. The supernatant was discarded, whereas the pellet was resuspended in PBS for analysis.

   For the preparation of fraction 2 (centrifugation-F2) 100 µl of initial stressed sample was overlaid on the top of 1.7 ml glycerol solution (25% w/w) using a pipette. The first centrifugation step was performed for 240 s at 50×g. The supernatant was collected in an eppendorf tube and centrifuged again for 220 s at 50×g. The resulting pellet was resuspended in PBS.

   For the preparation of fraction 3 (centrifugation-F3), 1 ml of the initial stressed sample was centrifuged for 60 s at 805×g. After centrifugation the supernatant was collected and analyzed.

   Fraction 4 (centrifugation-F4) was obtained by centrifuging 1 ml of centrifugation-F3 for 7 min at 1811×g. The supernatant was then collected for analysis.
2) Design of Experiments: Optimizing empirical parameters and refining fractionation

   The experimental parameters to obtain fraction 1–4 were refined using Central Composite Face-Centered Designs (CCF) of experiment. The optimization for each fraction is described in detail in the supporting information.

Preparation of Subvisible Particles by Preparative Flow Cytometry (FACS)

A BD FACS Aria IIu preparative cell sorter (BD Biosciences, San Jose, California) was used with BD FACSDiva v 6.1 software, applying the low-angle FSC detector equipped with a 488/10 bandpass filter for the 488 nm laser. A flow cytometry size calibration kit (1, 2, 4, 6 10, and 15 µm) from Molecular Probes (#F-13838; Life Technologies, Zug, Switzerland) with non-fluorescent microspheres was used for the calibration and definition of the sorting gates. For all experiments, autoclaved PBS (pH 7.2) was used as sheath fluid, prepared using 10× stock solutions and deionized water. To eliminate contaminating particles from the sheath fluid, the sheath line was equipped with 0.22 µm filter. Five milliliter 12×75 mm polypropylene round-bottom tubes (#352063, Corning Inc.) were used for fraction collection. All samples were filtered through 40 µm cell strainer (#352235, Corning Inc.) before sorting.

Size Exclusion Chromatography (SE-HPLC)

Samples were analyzed by UV absorbance detection at 280 nm. A TSK G3000 SWXL column (5 µm, 250 Å, 7.8× 300 mm) from Tosoh was used for separation. The mobile phase (200 mM sodium phosphate, 250 mM KCl, pH 7.0) was pumped at a flow rate of 0.5 mL/min. Sample size for analysis was 25 µg. The stationary phase was kept at 25±2°C. 1 ml of each sample was centrifuged for 10 min at 14,000 rpm before injection of the obtained supernatant. For each sample 25 µl was injected.

Light Obscuration

A HIAC ROYCO instrument model 9703 (Pacific scientific, New Jersey, USA) was used for all light obscuration (LO) measurements. A small volume method using a rinsing volume of 0.4 ml and 4 runs of 0.4 ml each was applied, as described previously (14). Flow rate was set to 10 mL/min. The first run was discarded and the average±standard deviation of the last 3 runs was reported for each sample. Blank measurements were performed at the beginning of the measurements and in between samples using fresh particle-free water. The acceptance criterion for blanks was: "less than 5 particles>1 µm". The system suitability test consisted of the measurement of count standards of 5 µm (Thermo Fisher count standards) with acceptance limits of±10% the reported concentration for particles bigger than 3.0 µm was performed in the beginning of each measurement day.

Flow Imaging Microscopy

The initial samples as well as all collected fractions were analyzed by flow imaging microscopy (FI) using a MFI DPA4200

series instrument (ProteinSimple, Santa Clara, California) equipped with a 470 nm LED light source. All particles larger than 1 μm in equivalent circular diameter were reported, considering the lower limit of detection of equipment. Size and count standards (ThermoFisher, Reinach, Switzerland) were used to check consistency of the sizing and counting accuracy of the instrument on the day of each measurement. The system was cleaned (before each measurement day) using 1% (w/v) Terg-a-zyme® (Sigma Aldrich, St. Louis, Missouri), followed by rinsing with water for 10 min. For these flushing steps, the flow rate was set to "maximum speed". Flushing with water was repeated after each sample. The "optimization of illumination" routine was performed prior to analysis, using filtered sample or PBS matching the buffer composition of the sample to be analyzed (*e.g.*, filtered sample for measuring after heat stress or PBS to measure FACS fractions). For measuring, 1 ml of sample was placed in a 1 ml dual-filter tip on the inlet port.

Resonant Mass Measurement (RMM, Archimedes)

Resonant Mass Measurements (RMM) were performed using Archimedes system (RMM0017, generation 2) from Malvern instruments LTD (Malvern, United Kingdom). Micro sensor chips with internal microchannel dimensions of 8 μm × 8 μm were used for all the experiments. The calibration of the sensor was done using 1 μm Duke polystyrene size standards (Waltham, Massachusetts, USA) diluted in water to approximately 10^6 part/ml. The calibration was finalized after 300 particles were detected as recommended by the manufacturer. The particle density for proteinaceous particles was defined as 1.28 g/ml. Before measurement, one ml of the sample to be analyzed was centrifuged 5 min at 1258 × g in order to remove large particles that could block the sensor during RMM. The influence of the additional centrifugation step on the particle concentration can be seen in Supplemental Figure 7. Measurements were performed in triplicates and the sensor was filled with fresh sample during 40 s before each measurement. The limit of detection (also called threshold) was manually set to 0.015 Hz for each analysis. Each measurement stopped either after 1 h of measurement or when a total of 4000 particles were detected. During measurement, the "autoreplenish" function was automatically activated every 500 for 5 s to load fresh sample and avoid settling down of particles in the sensor and tubings.

RESULTS

The aim of this study was the development, comprehensive evaluation and comparison of methods for the preparative fractionation of proteinaceous subvisible particles, with diameters ranging from hundreds of nanometers to approximately hundred micrometers. Two different methods were evaluated. Besides the two reported methods, other techniques such as sequential filtration, gravitation, asymmetrical flow field-flow fractionation or gel chromatography were initially also tested for their applicability to isolate different size fractions. However, these methods had limitations in their usable size range or sample amount.

First, a differential centrifugation fractionation of proteinaceous particles was developed and carried out to obtain a number of discrete fractions of various sizes spanning the range mentioned earlier. In order to optimize the method and process parameters, a statistical design of experiments approach (DoE) was applied. Second, fractionation of proteinaceous particles using preparative FACS strategy, comparable to the method reported elsewhere (20), was applied. The factors influencing the quality of separation in both methods were examined in detail. Light obscuration (LO), Flow Imaging (FI), flow cytometry and Resonant Mass Measurements (RMM) were used to measure the particle size distributions of the resulting fractions. The digital images generated by the FI measurements allowed an approximate calculation of ratio of protein particles contained in these fractions. RMM was used for the detection and quantification of submicron particles.

Generation and Characterization of Subvisible Proteinaceous Particles

In order to generate sufficient amounts of proteinaceous particles for method assessment, a starting solution of therapeutic IgG1 protein product with concentration of 25 mg/ml was heated to 80°C for 3 min which lead to the extensive particle formation. After this treatment, the relative protein monomer content in the supernatant was below 0.05% and no nanometer aggregate formation could be detected by size exclusion chromatography. After heat stress, the resulting samples contained particles in a broad size range (see Fig. 1a). The harsh treatment described above generated numerous very large particles which were broken up into smaller species by drawing and pushing these through a 27G × 1.5"needle mounted on a 5 ml disposable syringe, resulting in a typical decay distribution with increasing size (see also Fig. 1b). The proteinaceous particles prepared using this technique demonstrated adequate stability upon dilution in PBS and in the media used in all experiments (measured by flow imaging microscopy—see Supplemental Figure 8). Furthermore, the particles produced using the procedure described above were sufficiently stable upon freeze/thaw and storage at −80°C (Supplemental Figure 8), to allow sample storage.

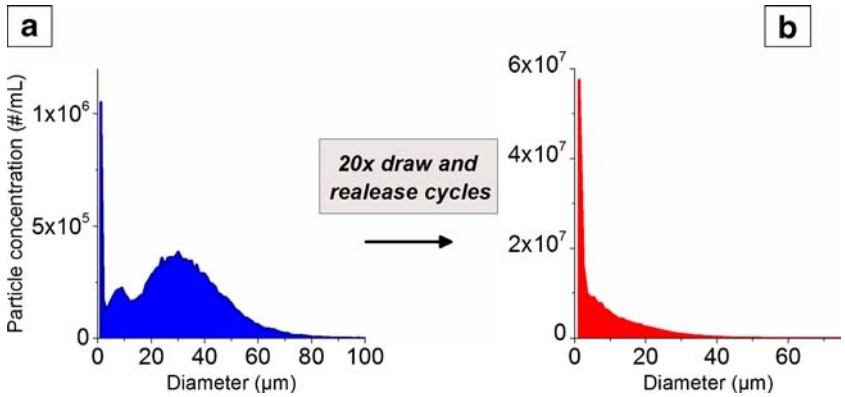

Fig. 1 Size-distribution obtained suing MFI of the sample after heat/shake stress (**a**) and consequent application of 20 syringe draw and release cycles (**b**).

Fractionation of Subvisible Proteinaceous Particles Using Differential Centrifugation

An empirical approach for centrifugation using adapted Stokes law [$T = 9\ln/(2r^2(\rho_p - \rho_s)\omega^2 R]$ where T represents the centrifugation time, r is the radius of a sphere, ρ_p is the density of the particle, ρ_s stands for the density of the solution, ω is the angular velocity of the centrifuge and R is the rotor radius, was used to isolate four different fractions of high purity (approximate mean diameters; 0.4, 1.5, 15 and 40 µm). These experiments informed the definition of the critical experimental parameters that might have an impact on the fractionation performance.

In order to extend centrifugation times to practical length, to slow down the sedimentation of large particles and prevent co-sedimentation of particles of different sizes, we noticed that it was necessary to increase the viscosity of the medium. This was achieved by the addition of glycerol to varying concentrations (see Table I). A content of 25% glycerol (w/w) was sufficient to maintain large particles (>15 µm) in suspension and avoid rapid sedimentation. To verify that the use of glycerol did not impact the morphology of the particles flow imaging microscopy measurements were carried out. Indeed, particles which were in contact with glycerol during the fractionation procedure and consequently resuspended in PBS did not show any measurable difference in their size, circularity, aspect ratio and object intensity parameters in comparison to particles that did not have contact with glycerol (data not shown). Moreover, the amount of glycerol remaining after centrifugation and resuspension of pellets in PBS was estimated (based on pellet/fraction volumes) to be relatively low (approximately 2.5% (w/w)). To arrive at these initial parameters for the empirical approach, a broad screen was carried out in a large number (~1000) of experiments which explored the following parameter ranges: centrifugation time in the range of 30 s–6 h, acceleration in the range of 8–3226 × g, and glycerol concentrations from 0 to 100% . As a guide to future experiments, we would suggest the user to begin with the parameters outlined in Table I . and adapt them in order to fulfill their requirements.

In a second step, a design of experiments (DoE)-approach was used to further optimize and refine the fractionation parameters. For this approach a response surface methodology (RSM) and a Central Composite Face-Centered Designs (CCF) were utilized due to their flexibility, efficiency and the fact that the experiments could be run sequentially. The empirically optimized fractionation parameters in the first step of the method development served as center points of each DoE. The aims of the DoE optimization (optimal responses) were high purity and high particle concentration in the desired size range. Therefore, the variables (*i.e.*, acceleration, centrifugation time and glycerol concentration) and responses were selected in each case as described in Table I. Each optimal point was confirmed experimentally to verify the predicted optimal conditions. After each successful confirmatory run the respective fractionation using those optimal conditions was repeated in larger scale in order to perform the full analytical characterization (SE-HPLC, RMM, FI, LO).

Using the DoE optimization it was possible to refine the experimental parameters in order to obtain higher particle concentration and/or reach size targets for four different fractions as described in Table I and Fig. 2. The proportion of the variation of the response described by the model (R2) shows in all the cases that the data was accurately modeled (see Supplemental Figure 2B, Supplemental Figure 3B, Supplemental Figure 4B, and Supplemental Figure 5B). The high values obtained for the proportion of the variation of the response predicted by the model according to cross validation (Q2) allow good model prediction in each case. Moreover, the models were deemed to be valid as demonstrated by validity values larger than 0.25 for each model (indicating no lack of fit) as depicted in supplemental figure 2B to 5B.

The size distributions of the four DoE optimized fractions described above were measured using LO and the additional characterization methods FI and RMM (see Fig. 2). Besides the minor discrepancy between the distributions reported by LO and flow imaging microscopy (observations also previously reported in literature (32,33)) the results presented in Fig. 2 demonstrate that the resulting fractions had high particle concentrations in the targeted size ranges, high purity as indicated

Table I Centrifugation parameters to obtain four different fractions, including final results obtained with empirical approach and optimized results using a DoE. Techniques used to measure individual fractions: *MFI* Microflow Flow Imaging and *RMM* Resonance Mass Measurement

Name	Target/ mean size expected	Process	Variables for centrifugation: time, acceleration, and glycerol concentration	Particle concentration [#/ml]	Mean diameter measured in μm	Comments
Centrifugation-F1	Larger than 40 μm	Empirical	180 s-25 × g-25%	1.5×10^5 (MFI)	38.1 (MFI)	Higher particle concentration and larger mean diameter
		Optimized by DoE	200 s-48 × g-26.8%	1.6×10^5 (MFI)	42.3 (MFI)	
Centrifugation-F2	15 μm	Empirical	240 s-50 × g-25% + 220 s-50 × g	1.5×10^5 (MFI)	17.8 (MFI)	Lower particle concentration for particle larger than 25 μm
		Optimized by DoE	260 s-72 × g-25% + 180 s-72 × g	1.5×10^5 (MFI)	15.3 (MFI)	
Centrifugation-F3	Close to 1 μm	Empirical	60 s-805 × g	8.0×10^5 (MFI)	1.33 (MFI)	Lower particle concentration but smaller mean diameter (*i.e.*, lower amount of bigger particles)
		Optimized by DoE	160 s-846 × g	4.2×10^5 (MFI)	1.25 (MFI)	
Centrifugation-F4	Smaller than 0.5 μm	Empirical	7 min-2051 × g	4.1×10^6 (RMM)	0.43 (RMM)	Lower particle concentration but smaller mean diameter (*i.e.*, lower amount of bigger particles)
		Optimized by DoE	11 min-2465 × g	2.1×10^6 (RMM)	0.36 (RMM)	

by low content of small particles in large fractions (centrifugation-F1 and centrifugation-F2) and low content of large particles in the small fractions (centrifugation-F3 and centrifugation-F4). Representative FI images of particles from the different fractions can be found in Supplemental Figure 6.

As seen in Fig. 2, defining features (and major advantages) of the differential centrifugation approach were: a) the relatively high concentrations of particles that can be achieved in the final fractions and b) the broad size range that can be accessed using this method. Resuspension of the pellet (for fractions containing large particles) allowed adjusting the particle concentration and the buffer composition to user requirements. Moreover, contamination of large size fraction with nanoparticles was nearly completely eliminated by adding glycerol during the centrifugation process.

Fractionation of Subvisible Proteinaceous Particles Using FACS

For the preparation of micrometer-sized subvisible proteinaceous particles, the same starting material was used as for the centrifugation approach (see Materials and Methods section). In principle, preparation of nanometer-sized particle fractions by FACS is also possible, although using this approach restricts the sample to low final protein concentrations. These low concentrations may present challenges for follow-up biological characterization studies. The sizes of the target fractions were estimated using a FACS size calibration kit containing beads with an approximate diameter of 2, 4, 6 and 15 μm and the Forward Scatter (FSC-A) signal. The cell sorter used in this study (see Materials and Methods section) allows simultaneous sorting of four different size-fractions. The position and the broadness of gates were set to achieve very narrow size-fractions (see Figs. 3 and 4.). However, it needs to be pointed out that narrow gates require more material and longer sorting times (see Supplemental Figure 1). The particles were sorted (with settings "four-way purity") applying the gate limits defined above. After sorting, all fractions were measured using flow cytometry (see Fig. 3.) The polystyrene beads, as well as the sorted proteinaceous particles where measured using FI (for representative images see Fig. 3 b and c). As seen in Figs. 3 and 4 all fractions were in excellent agreement with the polystyrene beads of similar size and the final size distributions matched the pre-determined gates which was confirmed by the additional analytical methods applied.

The first experimental parameter explored in detail was the nozzle size. Using different nozzle sizes influenced the particle concentration of the sorted fractions. As expected, larger nozzle sizes lead to larger drops containing more sheath fluid (PBS) and sample buffer (also PBS). Thus, the risk of coincidence of two or more particles per drop is higher for larger drops and the drop frequency is much lower compared to streams from smaller nozzles. In addition, larger nozzle sizes require less pressure and exert a less harsh mechanical treatment to particles. Conversely, some of the disadvantages of smaller nozzle size are the higher tendency for clogging of the orifice and also spraying of the stream by partial blocking and the resulting diversion of the stream. Larger particles may cause a deflection of the stream by partial blocking the nozzle and therefore mis-sorting when passing through the nozzle.

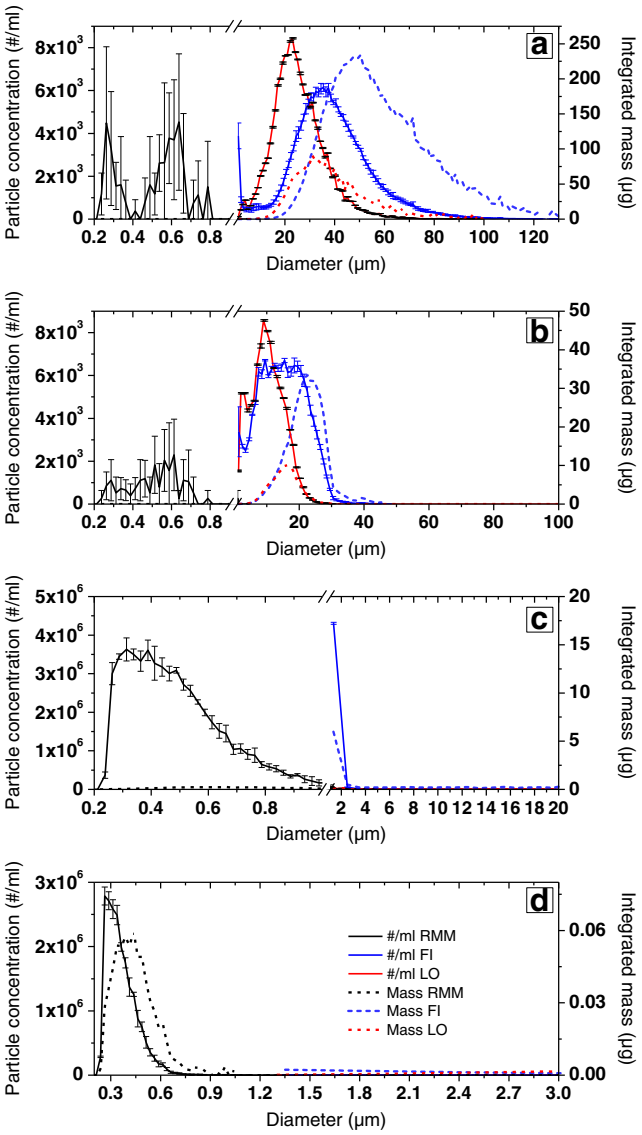

Fig. 2 Particle concentration (*solid lines*) and integrated mass (*dashed lines*; see Materials and Methods for detailed description of the calculations) for fraction 1 (**a**), fraction 2 (**b**), fraction 3 (**c**), fraction 4 (**d**) obtained by centrifugation with optimized conditions. Results from RMM are shown in *black*, FI measurements in *blue* and LO - in *red*.

After testing all three available nozzles, the 100 µm nozzle was chosen as optimal for the target fractions, because it applied the softest conditions in matters of pressure and mechanical stress from passing the nozzle.

The optimal number of events per second (*i.e.*, number of particles) in FACS is a quarter of the overall drops per second (manufacturer's recommendation). Therefore, in the case of the 70 µm nozzle with a drop rate of 90 kHz, the optimal rate is ~22,000 events/s and for the 100 µm nozzle with a drop rate of 30 kHz the optimal rate is ~7500 events/s. In cases where higher concentrations of particles in the starting solution were used, a higher discard rate of drops by the instrument was observed, which resulted in an increased probability of coincidence of two or more particles in one drop (not separated). Therefore, the concentrations of particles in the starting material were adjusted below 7500 events/s by dilution with PBS (sheath fluid). It needs to be pointed out that using a buffer different from the sheath fluid may lead to false positive results due to differences in the refractive indices or in rare cases foaming.

The resulting sorted fractions were analyzed using flow cytometry (Fig. 3a), LO and FI (to quantify the particles larger than 1 µm) and RMM for submicrometer particles (Fig. 4a–d). The results from all size-distribution measurements were consistent between all methods with a small shift to smaller sizes in the case of LO measurements. This minor undersizing effect has been described previously in reports that have reported smaller and fewer particles in LO as compared to flow imaging microscopy (32,33). The content of submicrometer particles in all four FACS fractions determined by RMM was several million particles per ml (Fig. 4). These smaller particles could not be measured and fractionated by FACS due to the technical limitation of this method to detect only scattered light of particles larger than the laser wavelength. All particles smaller than this threshold cannot be detected and end up in all FACS-sorted fractions. Therefore, after sorting, the samples did contain not only particles of the desired size but also a small amount of "contaminating" particles of smaller (submicrometer-sized) and larger sizes. This can be attributed either to a) the possible break-up or aggregation of particles upon sorting due to the mechanical forces that are applied apart, b) coincidence of two particles in one drop or c) partial blocking of the nozzle by large particles causing diversion of the stream. One strategy to increase the purity of the fractions is by resorting the already sorted fractions (20). However, it was found that resorting only led to a small increase in the purity, but in a large decrease in the concentration of particles. In comparison to a previous study (20), the purity of the individual initial fractions in the current report was very high and therefore, a resorting was not justified. The relatively high purity after the first sort was attributed to the higher stability of the particles as compared to the previous report. Data regarding the stability (reversibility) of fractions after freeze/thaw can be found in Supplemental Figure 8 (FACS fraction 1 and fractions generated by differential centrifugation given as examples). A comparison of the fractions generated by centrifugation and FACS can be found in Table II.

DISCUSSION

In this study a number of method attributes were evaluated in order to understand the applicability of the individual methods and define a toolkit for characterization of proteinaceous subvisible particles that researchers can use in future studies. The size-range, resolution, purity and yield and some additional factors were systematically assessed.

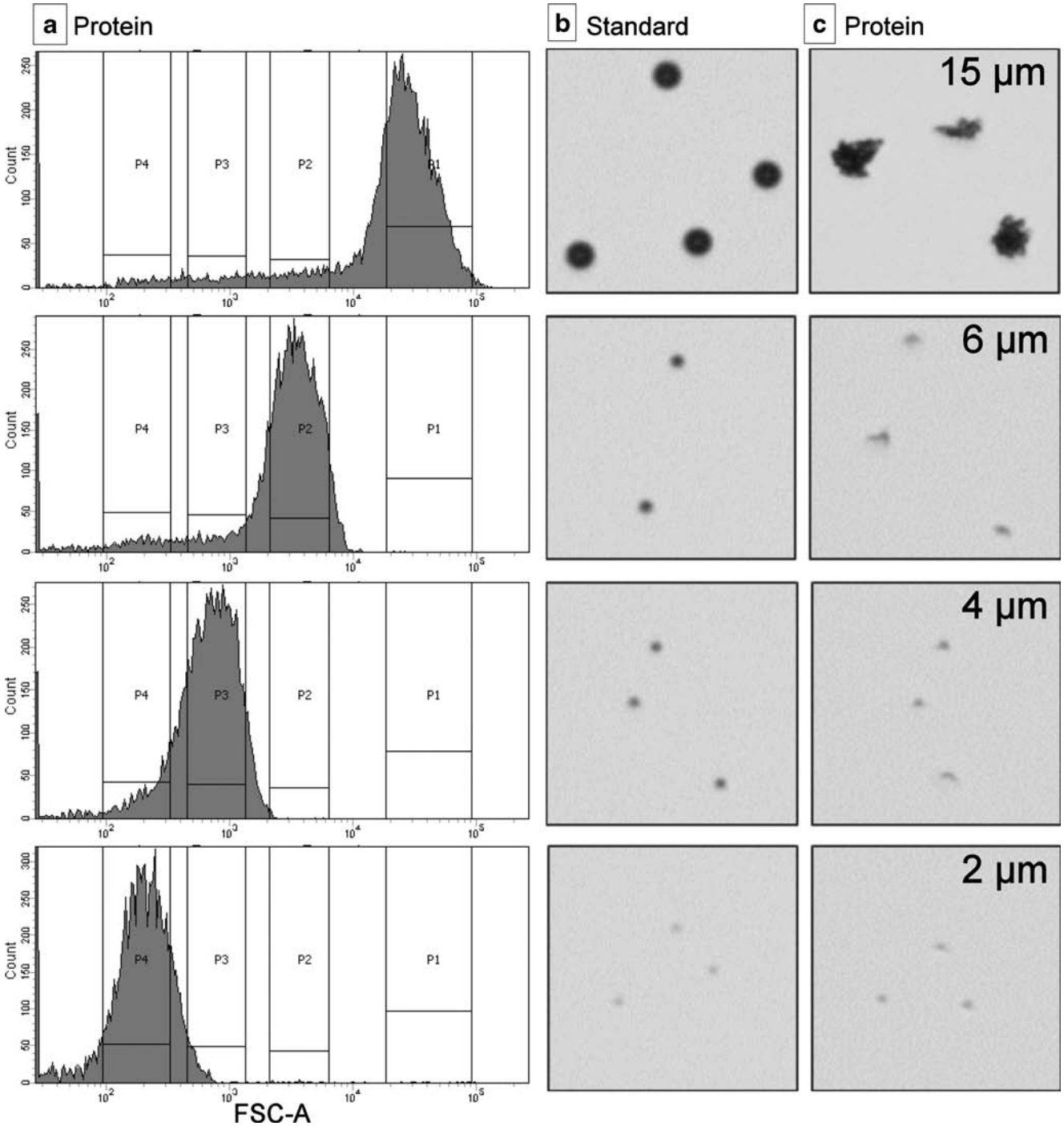

Fig. 3 Fractions sorted using FACS and reanalyzed with flow cytometry (**a**). Flow imaging microscopy images of the size-standards used in the FACS experiments for gate determination (**b**). Representative FI images of protein fractions after FACS sorting (**c**).

Size-Range

Naturally, both methods examined in this study are restricted in their working size-range by physical limitations related to the separation principle or the instrumentation used. For example, the smallest particles that FACS can theoretically separate have a diameter of 0.5 µm. The lower detection limit could in principle be improved by increasing the angle of the forward scattering (FSC) detectors because particles with sizes near and below the laser wavelength (nanometer-sized particles) scatter proportionally more light at larger angles (34). The limit is also dependent on the instruments settings for the detector voltage of the forward and side scatter detectors. It has been shown that detector voltage settings for

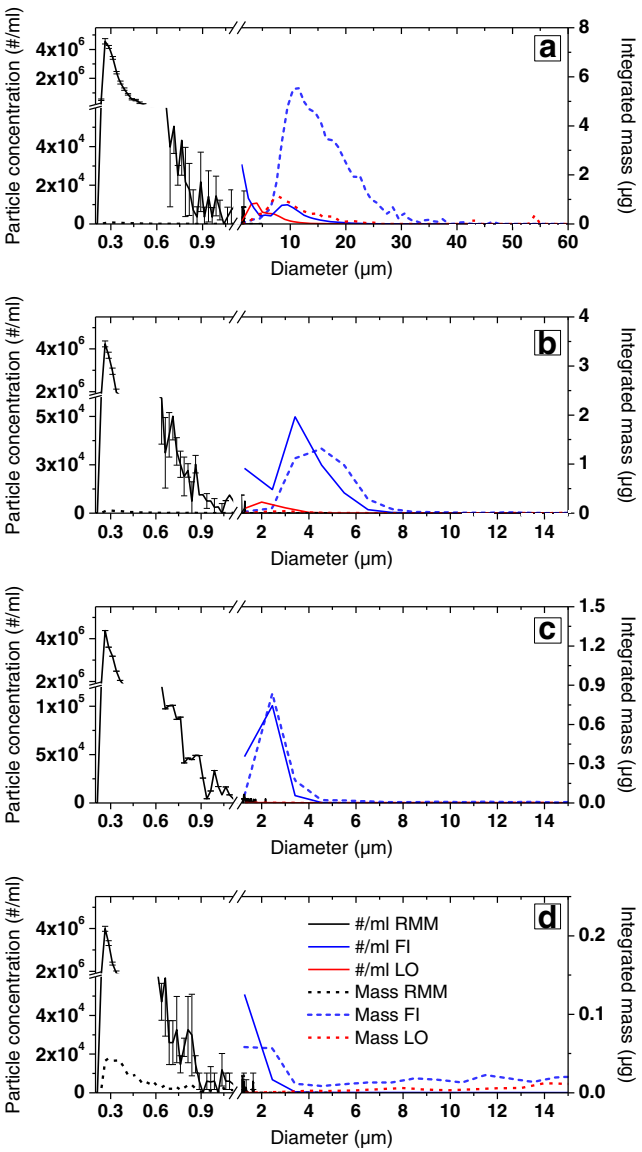

Fig. 4 Particle concentration (*solid lines*) and integrated mass (*dashed lines*; see Materials and Methods for details on calculation) for fraction 1 (**a**), fraction 2 (**b**), fraction 3 (**c**), fraction 4 (**d**) isolated by FACS. Results from RMM are shown in *black*, FI measurements in *blue* and LO - in *red*.

detection of very small particles (0.5 to 3 µm) are not suitable to distinguish between larger sizes (larger than 3 µm) and settings for larger particles (larger than 1 µm) results in the loss of sensitivity for particles smaller than 1 µm (35). The upper size-limit of FACS instruments is dependent on the nozzle size. As a general recommendation the manufacturer suggests not to exceed an object size of 50 µm for this specific instrument.

In contrast to FACS, centrifugation-based separations are less restricted in their working size-range. As a consequence, the differential centrifugation method described here can be used to preparatively separate a much broader size range of particles as compared to FACS-particles between the sizes of

Table II Summary for fractions isolated *via* centrifugation or FACS

Parameters	Centrifugation-FI	Centrifugation-F2	Centrifugation-F3	Centrifugation-F4	FACS-FI	FACS-FI	FACS-F3	FACS-F4
Flow imaging microscopy particles/ml (1–200 µm) ± SD	$2.0\times10^5\pm4.0\times10^3$	$1.5\times10^5\pm3.6\times10^3$	$4.4\times10^6\pm2.4\times10^4$	$1.6\times10^3\pm1.2\times10^1$	1.3×10^5	1.2×10^5	1.6×10^5	0.6×10^5
LO particles/ml(1.3-100 µm) ± SD	$1.7\times10^5\pm2\times10^3$	$1.1\times10^5\pm.5\times10^2$	$1.0\times10^5\pm2.4\times10^3$	$1.5\times10^2\pm1.4\times10^1$	$6.8\times10^4\pm6\times10^2$	$1.2\times10^5\pm1.8\times10^2$	$6.7\times10^2\pm2.9\times10^1$	$5.1\times10^2\pm2.7\times10^1$
RMM particles/ml(0.2-5 µm) ± SD	$4.0\times10^4\pm1.6\times10^4$	$2.0\times10^4\pm1.5\times10^4$	$1.0\times10^8\pm1.6\times10^4$	$2.1\times10^7\pm2.8\times10^5$	$1.7\times10^7\pm5.9\times10^5$	$2.4\times10^7\pm8.3\times10^5$	$1.9\times10^7\pm5.4\times10^5$	$2.1\times10^7\pm3.5\times10^5$
Mean diameter (µm) + (instrument used to measure)	38.8 µm (MFI)	15.3 µm (MFI)	1.25 µm (MFI)	0.36 µm (RMM)	13.1 µm (MFI)	4.5 µm (MFI)	2.3 µm (MFI)	1.6 µm (MFI)
Working fluid	PBS or placebo buffer	PBS or placebo buffer	PBS or placebo buffer	PBS or placebo buffer	PBS	PBS	PBS	PBS
Additives	Glycerol	Glycerol	none	none	none	none	none	none

0.2 and 100 μm can be easily separated. Therefore, one major advantage of differential centrifugation is its suitability for preparation of submicrometer particle fractions. In addition, as demonstrated in this study (see Fig. 2a), particles larger than 40 μm can be easily separated as well. The possibility to obtain particle fractions of different sizes ranging from low-nanometer to larger than 100 μm in the same experiment is a major advantage of differential centrifugation. However, it needs to be mentioned that obtaining multiple size-fractions in a single experiment requires the use of an additive to increase the viscosity of the medium (*i.e.*, glycerol or sucrose) in order to avoid cross-contamination of the different fractions.

Table III Comparison of the attributes of FACS and differential centrifugation methods with respect to the generation of micrometer-sized subvisible particle fractions

Attribute	Method	
	Differential centrifugation	FACS
Presence of nanoparticles	Low	High
Resolution	Medium	High
Yield	High	Low
Size range	Large	Medium
Preparation time	Long	Medium
Additives needed	Yes	No

Resolution

A major difference between both methods is the resolution of prepared fractions. With flow cytometry it was possible to prepare particles in a very narrow size window, *e.g.*, 2 μm (Fig. 4). The differential centrifugation method allowed isolating fractions with approximate mean diameters of 0.4 μm [0.2–0.8 μm], 1.5 μm [0.2–2.5 μm], 15 μm [1–30 μm] and 40 μm [10–60 μm], whereas FACS fractionation method separated fractions with mean diameters of 2 μm, [1–3 μm] 4 μm [3–5 μm], 6 μm [5–7 μm] and 15 μm [5–25 μm]. With exception for sub-micron fractions, the centrifugation method generated rather broad size distributions. For example, comparison of the 15 μm fractions generated by FACS (Fraction 1, Fig. 4a) and differential centrifugation (Fraction 2, Fig. 2b) show a very broad distribution for the fraction using the second method. In contrast, the 15 μm fraction generated by flow cytometry was much narrower in size range. Very narrow fractions of 2, 4 or 6 μm mean particle diameter have also been generated using FACS, which was not possible with the centrifugation method. Whereas obtaining fractions of discrete sizes using centrifugation was challenging and might need further development. In principle, the FACS method can be used to generate even more narrow fractions than the ones reported here. Naturally, one drawback associated with such efforts would be the requirement for more material and longer fractionation run times. The time for sample preparation with both methods is very different and depends highly on the initial sample and its preparation. As stated in Table III, differential centrifugation uses more time than FACS mainly because of the higher sample amount requirements. The fractionation run time (*i.e.*, the instrument time that was needed for either centrifugation or FACS, not counting the time for sample preparation or setup of the instrument) for 1 ml of both 15 μm fractions is 8 min for centrifugation and 5 min with FACS. Any changes in size range of the desired fraction and particle concentration of the initial sample can significantly change these time frames.

Purity and Yield

One drawback of the FACS fractionation method is the inability to detect particles smaller than 0.5 μm due to physical limitations in the detection with laser light scattering. This leads to contamination of all FACS fractions with small particles which can be detected using alternative methods (*e.g.*, RMM, FI). Indeed, RMM confirmed the presence of nanoparticle contaminants in the FACS fractions (Fig. 4a–d). Although, resorting of the initial fractions did minimize the nanoparticle contamination, the improvement was attributed largely to the dilution effect rather than specific removal of submicrometer particles. More importantly, the differential centrifugation method does not have this limitation. Figure 2a and b show a very low content of submicrometer particles in the micrometer fractions (Fraction 1 and 2). This also suggests an interesting approach to achieve very pure and also narrowly sized fractions—a combination between FACS and centrifugation fractionation. More specifically, a first-pass centrifugation step could be applied to remove the nanoparticles present in a sample. As a second step the micrometer centrifugation fractions can be separated using FACS to generate well-defined fractions of specific sizes. Alternatively, the approach can be reversed centrifuging FACS-generated fractions to separate micrometer from nanometer particles. However, the latter approach may be impractical due to the necessity for viscosity additives (*e.g.*, glycerol).

Although some of the fractions generated in this study did contain certain amounts of "contaminating" nanoparticles, if calculated in terms of protein mass the impact of this contamination was negligible. Flow imaging microscopy and RMM data can be used to perform such calculations of the total protein mass of the particles present in every sample based on the digital image analysis (taken in Flow imaging microscopy) (36) or on the buoyant mass (RMM) (37). Such calculations for the fractionation experiments presented here showed practically no influence of the submicrometer particles on the protein content of micrometer fractions generated by FACS

and centrifugation (Figs. 4a–d and 2a–b). However, the mass calculations reveal an important practical aspect of the fractionation of subvisible particles—*i.e.*, the fractions of the smaller-sized particles contain much less protein than the larger-sized fractions. This effect is a natural consequence of the power relationship between size and volume (*e.g.*, sphere $= \frac{4}{3}\pi r^3$). Interestingly, the impact of this effect seems to be larger in the FACS fractionation method, which can be attributed to the higher purity of the individual fractions.

The particle concentration generated by FACS is limited by the fact that the flow cytometer sorts drops of buffer and sheath fluid of the same size. Drops with smaller particles therefore, contain relatively more sample fluid than large drops that almost fill out the whole drop. This can also be seen at the particle concentration measured by FI of the FACS fractions 1 to 3 indicating that the same number of particles is present in the same volume. Fraction 4 has a lower particle concentration due to the detection limit of the FI instrument. Therefore, FACS cannot be used to create concentrated fractions, but might be combined with centrifugation to concentrate and also to remove submicron contamination from the fractions as described above. Using centrifugation it would be possible to reach even larger protein concentrations (than those presented here) for fractions including the resuspension of a pellet (Fraction 1 and 2). Indeed, each pellet was resuspended in 1 ml of PBS in our study but for some other purposes the number of pellets or the initial volume could have been increased and resuspended in smaller volumes (data not shown). Although the primary target was purity of the fractions, we calculated the recovery yield for both 15 μm fractions generated with FACS and centrifugation. The initial sample contains 86 million particles/ml in the size range between 5 and 25 μm which is diluted 1 to 5. The FACS fraction 1 contains only 60,000 particles/ml, *i.e.*, 0.35%. For centrifugation fraction 2 the initial sample was diluted 1 to 10 and contains 150,000 particles/ml, *i.e.*, 1.75%. However it needs to be pointed out that 1 ml of initial sample yields more than 1 ml after FACS sorting.

Other Factors

An important consideration in setting up fractionation of subvisible particles using the methods described in this study is the particle concentration in the samples. For example, in flow cytometry the number of particles should not exceed the number of drops per second (*e.g.*, 7500 events per sec with the 100 μm nozzle) in order to avoid coincidence of two or more particles in the same drop. Thus, high particle concentrations can lead to either mis-sorting and/or to slower sorting rates because of discarded drops containing multiple particles. In the case of centrifugation we only tested experiments using protein solutions with concentrations of up to 25 mg/ml. It is conceivable, that higher concentrations might need to be diluted before centrifugation to prevent an interaction between large and small particles.

The centrifugation-based approach to fractionation of particles larger than 5 μm requires the addition of viscosity modifiers (*e.g.*, glycerol) to reduce the sedimentation speed and improve the fraction purity. In fact, it is exceedingly difficult to isolate proteinaceous particle fractions of large mean diameter (*e.g.*, 30–40 μm) without the use of glycerol. Our first attempts to generate such fractions without glycerol always contained a large number of smaller particles (0.2 to 2 μm). Of course, the use of glycerol may potentially result in additional complications—for example, the addition of glycerol may induce changes in the particle size- or morphology distributions. This was not the case in the experiments reported here and such changes were not observed or reported in the literature, but it remains a theoretical possibility which needs to be carefully controlled. A further practical aspect of the use of glycerol for fractionation by centrifugation is the fact that small amounts of glycerol are carried over after resuspension of the fraction pellet into working medium (buffer) resulting in the presence of glycerol in the final fractions (albeit in very low concentrations, *i.e.*, 2.5% w/w). Conversely, for the preparation of FACS fractions no additives are necessary, which may be an additional factor in choosing a fractionation method. The dilution of the samples fractioned by FACS can be done using any buffer, which in turn can be used as a sheath fluid in the FACS instrument with the only caveats that the buffer should not foam and needs to contain a sufficient amount of ions for charging and deflection.

Another major difference between both methods is the type of physical stress that is applied to the particles during the fractionation process. During centrifugation the samples experience centrifugal forces and perhaps shear stress, during flow cytometry fractionation several different types of stress are present. For example, in the flow cell a pressure of up to 70 psi (4.82 bar) is applied (depending on the nozzle size), which could impact the sample in either way. It has been reported that high pressure can be used to dissociate aggregates and refold protein, however, the pressure used in that study was significantly higher (2000 bar) (38) and therefore such effect is likely irrelevant. In the flow cell of the flow cytometer the particles pass through laser beams and the surrounding liquid is repeatedly charged negative and positive using electrical potential of (+/−) 40 to 80 V. After exiting the flow cell, the particles pass through a small orifice and return to atmospheric pressure, experiencing shear and cavitational forces. Afterwards, the sample is accelerated to 20 m/s and passes through an electric field of 3 to 5 kV/cm before hitting a liquid surface or a solid tube wall. There are alternative cell sorters available that divert the particles mechanically or by an air stream instead of electrostatics, but

these instruments have a maximal drop rate of 2 kHz and therefore 10 fold slower than the instrumentation used in this study. As a side note an instrument using air stream (Union Biometrica, Inc.) for sorting is capable to sort particles up to 1500 μm as advertised by the manufacturer. In relation to the physical stress it needs to be mentioned that the stability of the particles to be fractionated (their ability to remain intact, *i.e.*, irreversibility) is important. Although particle stability in FACS sorting was shown for stir stress (31) as well as syringe shear-cavitation stress (20), particles generated under different conditions with other proteins might demonstrate different stability behavior. For example, our experience with particles of the same IgG used in this study produced by stir stress was that they were not suitable to create fractions larger than 5 μm because these particles were fragile for this particular protein and this particular stress condition.

All technical challenges of mechanical, electrical or chemical nature mentioned above may have impact on the proteinaceous particles. Depending on the further use of the generated fractions, (*e.g.*, *in vivo* or *in vitro* biological assays) it might be necessary to assess possible physico-chemical changes induced by the separation process, particularly if the protein is sensitive to the types of stress exerted during fractionation. In such cases, additional investigations should be taken into consideration. It is recommended to consider CE-SDS to check degradation and covalent linkage, and RP-HPLC and peptide mapping to check for modifications like oxidation or deamidation of amino acid residues (39). Furthermore, it may be relevant to assess potential changes in the secondary and tertiary structure using spectroscopic techniques such as circular dichroism (CD), Fourier transform infrared- (FTIR), Fluorescence- or Raman spectroscopy. For the subsequent use in *in vivo* or *in vitro* assays it may also be important to check the endotoxin content. In principle both methods can produce fractions that have low endotoxin content if the necessary precautions are taken. A procedure to prepare a FACS for endotoxin-free sorting has been published recently (31) and is also available from some instrument manufacturers (*e.g.*, BD: prepare for aseptic sort). Finally, it should be pointed out that irrespective of the separation method particle size-fractions though enriched in size may still contain conformationally or chemically heterogeneous populations.

CONCLUSION

Here we report a comprehensive evaluation and optimization of the experimental parameters of two new methods for fractionation of proteinaceous subvisible particles of sizes between approximately 0.2 μm and 100 μm: differential centrifugation and FACS. Applying the optimized method parameters size-fractions of proteinaceous subvisible particles were isolated using both techniques and the methods' attributes such as size-range, resolution, fraction purity and yield were assessed. It was found that both techniques present advantages and disadvantages (see Table III for a summary) and will likely find complementary use in the research practice. Further research will focus on assessing immunogenicity in *in vitro* models of various fractions of protein aggregates and particles.

ACKNOWLEDGMENTS AND DISCLOSURES

We thank Tarik Khan for editorial help, Gabriela Quebatte and Adeline Boillon for helpful discussions and Marc Bedoucha for providing access to instrumentation and technical assistance.

REFERENCES

1. Rosenberg AS. Effects of protein aggregates: an immunologic perspective. AAPS J. 2006;8:E501–507.
2. Singh SK, Afonina N, Awwad M, Bechtold-Peters K, Blue JT, Chou D, *et al.* An industry perspective on the monitoring of subvisible particles as a quality attribute for protein therapeutics. J Pharm Sci. 2010;99:3302–21.
3. Carpenter JF, Randolph TW, Jiskoot W, Crommelin DJ, Middaugh CR, Winter G, *et al.* Overlooking subvisible particles in therapeutic protein products: gaps that may compromise product quality. J Pharm Sci. 2009;98:1201–5.
4. den Engelsman J, Garidel P, Smulders R, Koll H, Smith B, Bassarab S, *et al.* Strategies for the assessment of protein aggregates in pharmaceutical biotech product development. Pharm Res. 2011;28:920–33.
5. Singh SK. Impact of product-related factors on immunogenicity of biotherapeutics. J Pharm Sci. 2011;100:354–87.
6. Joubert MK, Hokom M, Eakin C, Zhou L, Deshpande M, Baker MP, *et al.* Highly aggregated antibody therapeutics can enhance the in vitro innate and late-stage T-cell immune responses. J Biol Chem. 2012;287:25266–79.
7. van Beers MM, Sauerborn M, Gilli F, Brinks V, Schellekens H, Jiskoot W. Oxidized and aggregated recombinant human interferon beta is immunogenic in human interferon beta transgenic mice. Pharm Res. 2011;28:2393–402.
8. van Beers MM, Gilli F, Schellekens H, Randolph TW, Jiskoot W. Immunogenicity of recombinant human interferon beta interacting with particles of glass, metal, and polystyrene. J Pharm Sci. 2012;101:187–99.
9. van Beers MM, Jiskoot W, Schellekens H. On the role of aggregates in the immunogenicity of recombinant human interferon beta in patients with multiple sclerosis. J Interferon Cytokine Res. 2010;30:767–75.
10. Mahler HC, Friess W, Grauschopf U, Kiese S. Protein aggregation: pathways, induction factors and analysis. J Pharm Sci. 2009;98:2909–34.
11. Joubert MK, Luo Q, Nashed-Samuel Y, Wypych J, Narhi LO. Classification and characterization of therapeutic antibody aggregates. J Biol Chem. 2011;286:25118–33.
12. Mahler HC, Müller R, Friess W, Delille A, Matheus S. Induction and analysis of aggregates in a liquid IgG1-antibody formulation. Eur J Pharm Biopharm. 2005;59:407–17.
13. Kiese S, Pappenberger A, Friess W, Mahler HC. Shaken, not stirred: mechanical stress testing of an IgG1 antibody. J Pharm Sci. 2008;97:4347–66.

14. Kiese S, Pappenberger A, Friess W, Mahler HC. Equilibrium studies of protein aggregates and homogeneous nucleation in protein formulation. J Pharm Sci. 2010;99:632–44.
15. Kükrer B, Filipe V, van Duijn E, Kasper PT, Vreeken RJ, Heck AJ, *et al.* Mass spectrometric analysis of intact human monoclonal antibody aggregates fractionated by size-exclusion chromatography. Pharm Res. 2010;27:2197–204.
16. Paul R, Graff-Meyer A, Stahlberg H, Lauer ME, Rufer AC, Beck H, *et al.* Structure and function of purified monoclonal antibody dimers induced by different stress conditions. Pharm Res. 2012;29:2047–59.
17. Hawe A, Romeijn S, Filipe V, Jiskoot W. Asymmetrical flow field-flow fractionation method for the analysis of submicron protein aggregates. J Pharm Sci. 2012;101:4129–39.
18. Johnand C, Langer K. Asymmetrical flow field-flow fractionation for human serum albumin based nanoparticle characterisation and a deeper insight into particle formation processes. J Chromatogr A. 2014;1346:97–106.
19. Freitag AJ, Shomali M, Michalakis S, Biel M, Siedler M, Kaymakcalan Z, *et al.* Investigation of the Immunogenicity of Different Types of Aggregates of a Murine Monoclonal Antibody in Mice. Pharm Res. 2015;32(2):430–44.
20. Rombach-Riegraf V, Allard C, Angevaare E, Matter A, Ossuli B, Strehl R, *et al.* Size fractionation of microscopic protein aggregates using a preparative fluorescence-activated cell sorter. J Pharm Sci. 2013;102:2128–35.
21. Lee YH, Tan HT, Chung MC. Subcellular fractionation methods and strategies for proteomics. Proteomics. 2010;10:3935–56.
22. Cahnand FH, Fox MS. Fractionation of transformable bacteria from competent cultures of *Bacillus subtilis* on renografin gradients. J Bacteriol. 1968;95:867–75.
23. Moni C, Derrien D, Hatton PJ, Zeller B, Kleber M. Density fractions versus size separates: does physical fractionation isolate functional soil compartments? Biogeosciences. 2012;9:5181–97.
24. Novak JP, Nickerson C, Franzen S, Feldheim DL. Purification of molecularly bridged metal nanoparticle arrays by centrifugation and size exclusion chromatography. Anal Chem. 2001;73:5758–61.
25. Sun X, Tabakman SM, Seo WS, Zhang L, Zhang G, Sherlock S, *et al.* Separation of nanoparticles in a density gradient: FeCo@C and gold nanocrystals. Angew Chem Int Ed Engl. 2009;48:939–42.
26. Nobleand PB, Cutts JH. Separation of blood leukocytes by Ficoll gradient. Can Vet J. 1967;8:110–1.
27. Lu Y, Ahmed S, Harari F, Vahter M. Impact of Ficoll density gradient centrifugation on major and trace element concentrations in erythrocytes and blood plasma. J Trace Elem Med Biol. 2015;29:249–54.
28. Jaatinen, T. and Laine J. Isolation of mononuclear cells from human cord blood by Ficoll-Paque density gradient. Curr Protoc Stem Cell Biol. Chapter 2:Unit 2A 1 (2007).
29. Lueders T, Manefield M, Friedrich MW. Enhanced sensitivity of DNA- and rRNA-based stable isotope probing by fractionation and quantitative analysis of isopycnic centrifugation gradients. Environ Microbiol. 2004;6:73–8.
30. Sohi SP, Mahieu N, Arah JRM, Powlson DS, Madari B, Gaunt JL. A procedure for isolating soil organic matter fractions suitable for modelling. Soil Sci Soc Am J. 2001;65:1121.
31. Telikepalli S, Shinogle HE, Thapa PS, Kim JH, Deshpande M, Jawa V, *et al.* Physical Characterization and In Vitro Biological Impact of Highly Aggregated Antibodies Separated into Size-Enriched Populations by Fluorescence-Activated Cell Sorting. J Pharm Sci. 2015;104:1575–91.
32. Werk T, Volkin DB, Mahler HC. Effect of solution properties on the counting and sizing of subvisible particle standards as measured by light obscuration and digital imaging methods. Eur J Pharm Sci. 2014;53:95–108.
33. Zhao, H., Diez, M., Koulov, A., Bozova, M., Bluemel, M., Forrer, K. Characterization of aggregates and particles using emerging techniques. analysis of aggregates and particles in protein pharmaceuticals. Wiley, 2012, 133–167.
34. Nolte-'t Hoen EN, van der Vlist EJ, Aalberts M, Mertens HC, Bosch BJ, Bartelink W, *et al.* Quantitative and qualitative flow cytometric analysis of nanosized cell-derived membrane vesicles. Nanomedicine. 2012;8:712–20.
35. Nishi H, Mathäs R, Fürst R, Winter G. Label-free flow cytometry analysis of subvisible aggregates in liquid IgG1 antibody formulations. J Pharm Sci. 2014;103:90–9.
36. Barnard JG, Singh S, Randolph TW, Carpenter JF. Subvisible particle counting provides a sensitive method of detecting and quantifying aggregation of monoclonal antibody caused by freeze-thawing: insights into the roles of particles in the protein aggregation pathway. J Pharm Sci. 2011;100:492–503.
37. Weinbuch D, Zölls S, Wiggenhorn M, Friess W, Winter G, Jiskoot W, *et al.* Micro-flow imaging and resonant mass measurement (archimedes) - complementary methods to quantitatively differentiate protein particles and silicone oil droplets. J Pharm Sci. 2013;102:2152–65.
38. Seefeldt MB, Rosendahl MS, Cleland JL, Hesterberg LK. Application of high hydrostatic pressure to dissociate aggregates and refold proteins. Curr Pharm Biotechnol. 2009;10:447–55.
39. Chirinoand AJ, Mire-Sluis A. Characterizing biological products and assessing comparability following manufacturing changes. Nat Biotechnol. 2004;22:1383–91.